

# Preparation of Polyaniline-Clay Nanoadditive and Investigation on Anticorrosion Performance in Epoxy Coating

Mohammadreza Bagherzadeh<sup>1\*</sup> and Mahdi Ghasemi<sup>2</sup>

<sup>1</sup> Nanotechnology and Carbon Research Group, Faculty of Downstream Petroleum Industry, Research Institute of Petroleum Industry (RIPI), Tehran, Iran

<sup>2</sup> Coating Research Group, Industrial Protection Research Division, Research Institute of Petroleum Industry, N.I.O.C., Tehran, Iran

## ABSTRACT

The corrosion protection of mild steel by a newly developed epoxy-based coating system containing inherently conducting nanopolyaniline-clay as a nanoadditive has been studied. Polyaniline-clay anticorrosion nanoadditive (PCNA) was obtained by the direct mixing method of nanopolyaniline (0.03 wt.%) and organo-modified clay (3 wt.%) at atmospheric pressure, and XRD technique was used to study *d*-spacing of clay platelets in the prepared nanoadditive. PCNA was dispersed in polyaminoamide hardener matrix and was used for epoxy coating (EPCNA) preparation. The particle size of the polyaniline in hardener was determined using dynamic light scattering technique (DLS). The results revealed that the particles were in the range of 50–58 nm. The degree of exfoliation and distribution and particles size were studied by XRD and TEM in the final dried film. The corrosion protection ability of EPCNA was compared to an epoxy coating containing pure nanopolyaniline (ENPN) using electrochemical impedance spectroscopy (EIS) and salt spray methods. In addition, an investigation on the morphology of metal-coating interface by scanning electron microscopy (SEM) technique in ENPN and EPCNA samples after salt spray test showed stable oxide layer formation for ENPN and a dense stable oxide layer for EPCNA on metal surface. The results showed that the PCNA nanoadditive enhanced corrosion protection effect in comparison to pure nanopolyaniline (NPN) in the epoxy coating.

**Keywords:** Nanoadditive, Nanopolyaniline, Nanoclay, Anticorrosion, Epoxy Coating, EIS

## INTRODUCTION

Additives are used to modify or improve the physical and mechanical properties of organic coatings. Nanoadditives are Nanoscale materials which have unique and potentially valuable properties in comparison to the same materials naturally existing on larger scales, which can

include greater tensile strength, enhanced electrical conductivity, and the ability to contribute to new chemical synthesis pathways. Indeed, adding nanoadditives to materials is a smart way that causes enhanced product properties like the improvement in surface coating corrosion protection behavior [1, 2].

With the advent of nanotechnology, especially in

### \*Corresponding author

Mohammadreza Bagherzadeh  
Email: bagherzadehmr@ripi.ir  
Tel: +98 21 4825 5384  
Fax: +98 21 4825 5384

### Article history

Received: June 23, 2014  
Received in revised form: September 01, 2014  
Accepted: November 12, 2014  
Available online: July 26, 2015

the area of the organic coatings, the application of nanoclay, polyaniline (PAni), and nanopolyaniline (NanoPAni) was highly interested. The primary research activities have been conducted on nanoclays due to their high interaction, environmental stability, good processability, and availability at low cost. Furthermore, because of physicomechanical and corrosion protection properties improvement, using nanoclays were considered in the manufacture of nanocomposite coatings [3, 4]. However, using additives was recommended for further improvement in the anticorrosive performance of polymer-clay nanocomposite coatings [3-6]. On the other hand, the conductive polymers (CP) such as polyaniline and its derivatives and also nanopolyaniline have been used as corrosion resistance promoter in organic coatings [5-8]. Therefore, more attention is paid to polyaniline-clay nanocomposite preparation and application as a surface coating such as thin film coatings for more corrosion protection [9-14].

Generally, polyaniline-clay nanocomposite preparation methods can be classified as follows [4, 5, 9, 10, 14-21]:

- direct mixing of polyaniline and clay;
- solution mixing of polyaniline and clay;
- In situ intercalative polymerization of polyaniline and clay;
- atmospheric in situ polymerization of polyaniline and clay;
- super critical in situ polymerization of polyaniline and clay.

First time, Yeh et al. [14] described the corrosion protection effect of nanocomposites based on polyaniline and organo-modified clay, which were synthesized via in situ polymerization. They concluded that polyaniline-clay nanocomposites in the form of coatings on cold-rolled steel were found much superior in corrosion protection compared to those of conventional polyaniline based on a series of electrochemical measurements.

In another research, the synthesis of hybrid polypyrrole-montmorillonite nanocomposites and their effects on the improvement to the epoxy coating protection on aluminum substrate were studied. The results showed that the incorporation of hybrid polypyrrole-montmorillonite nanocomposites into the epoxy resin increased the resistance of the prepared coating in comparison to neat epoxy, epoxy-clay, and epoxy-polypyrrole coatings [22].

An investigation on anticorrosion performance of nano- and micropolyaniline in water-based epoxy coatings has been reported previously [5]. The results showed that the coating containing nanopolyaniline had the best anticorrosion efficiency.

In this research, PAni-clay nanoadditive (PCNA) was prepared using NanoPAni and nanoclay by a direct mixing method. The prepared nanoadditive was used in epoxy coating to improve anticorrosion efficiency. For the preparation of hardener containing nanoparticles, PCNA and polyaminoamide hardener matrix were mixed and characterized by XRD technique in order to study the *d*-spacing of the clay platelets. Then, the prepared hardener was used in epoxy coating preparation. DLS technique and TEM were used for particle size analysis in hardener and the final dried film. In addition, the anticorrosion performance of the prepared coatings was studied by using salt spray and EIS test methods.

## EXPERIMENTAL PROCEDURES

### Materials

Epoxy resin was DGEBA (Epon 1001) from Shell Company and the Polyaminoamide hardener (Crayamid 115) was purchase from Cray Valley Company. The nanoclay was an organo-modified montmorillonite with a commercial grade of cloisite 30B, obtained from Southern Clay (Table 1) and the nanopolyaniline emeraldine salt (NanoPAni) with the trade name of ORMECON®

6312-119-001 was purchased from Ormecon GmbH (Table 2).

**Table 1: Organo-modified clay specification**

Property	Cloisite 30B
Color	Off white
Organic Modifier*	MT(EtOH) <sub>2</sub>
Modifier concentration (meq/100g clay)	90
Particle size (μ)	90% less than 13 μ
Density (g/cc)	1.98
d <sub>001</sub> (Å)	18.2

\* MT(EtOH)<sub>2</sub>: methyl, tallow, bis-2-hydroxyethyl, quaternary ammonium

**Table 2: Nanopolyaniline specification**

Property	Nanopolyaniline
Color	Dark green
Mixture form	Viscous liquid
Solid content	Approx. 12 %
Active component	Polyaniline (poly-phenylene-amine)
PAni content	Approx. 5.5 % in the mix
Solvents	Ethanol
Solvent content	Approx. 88 %
Particle size	30-150 nm

### PCNA Nanoadditive Preparation and Application

As a typical experiment for the preparation of PCNA nanoadditive with 3 wt.% clay and 0.03 wt.% NanoPAni loading (in resin and hardener mixture), 0.023 g NanoPAni were diluted with 20 ml butyl glycol and then sonicated for 3 minutes using an ultrasonic homogenizer (Hielscher UIP1000hd) and also 2.3 g cloisite 30B was dispersed in 50 ml butyl glycol separately. The prepared NanoPAni mixture was added to Cloisite 30B swelled in butyl glycol and homogenized for 5 minutes by a homogenizer (Polytron 6100 Kinematica) and then was sonicated for 20 minutes. The produced PCNA was added to the hardener and then, to have

smaller particles and a better size distribution, it was homogenized and sonicated for 15 and 35 minutes respectively. In this step, the polyaniline emeraldine salt was changed to emeraldine base and the color of the mixture changed to dark blue because of the basic media of the Crayamid 115 hardener.

### Preparation of Epoxy Coating Containing PCNA

The Coating was prepared by mixing the stoichiometric amount of hardener containing PCNA and epoxy resin (epoxy resin/hardener = 65/105) and then was mixed well for 10–15 min. Viscosity of the prepared coating was adjusted by solvent and then it was applied by air spray on the sand blasted mild steel samples. The coating was allowed to cure for 7 days at ambient condition before being subjected to various testing. Dry film thicknesses of the coatings were about 70±5 μm.

### Characterization

Wide-angle X-ray diffraction (WAXD) (Philips PW1840) was used for the measurement of the degree of exfoliation and *d*-spacing between the clay platelets. The size of polyaniline particles in hardener was measured via dynamic light scattering (DLS) technique using Pultron nanozetasizer. A Philips CM200 transmission electron microscopy (TEM) was used for the particle size measurement in EPCNA and ENPN and also distinguishing the dispersion of nanoparticles in final dry film. Scanning electron microscopy (SEM) (Hitachi S4160) was used for the observation of the metal-coating interface of the samples.

### Evaluation of Coating Corrosion Resistance Properties

#### Salt Spray Test

The study was carried out according to ASTM B117 standard. Mild steel panels with a size of 10 cm×15 cm×0.2 cm coated with EPCNA and

ENPN were placed in the salt spray chamber at an angle of  $15^\circ$  to horizontal. A 3.5 wt.% salt solution was prepared and sprayed by atomizer with a nozzle pressure of 10-12 psi. The coated panels were closely examined periodically for any surface change by visual inspection.

### Electrochemical Impedance Spectroscopy (EIS)

The electrochemical impedance measurements were performed on steel specimens with a size of  $5\text{ cm} \times 5\text{ cm} \times 0.2\text{ cm}$ . The plates were sandblasted (Sa 2.5) and degreased with acetone and then coated with the developed coating. A glass tube with a diameter and length of 2.26 cm and 5 cm respectively was fixed on the coated steel with adhesive and the area exposed to the solution was  $4.0\text{ cm}^2$ . The coated panels were exposed to a 3.5 wt.% NaCl electrolyte. The EIS measurements were performed in the glass tube, where a saturated calomel electrode (SCE) was the reference electrode, graphite was the counter electrode (CE), and the coated steel was the working electrode (WE). The assembly was connected to electrochemical impedance analyzer (Potentiostat/Galvanostat Model Autolab 302N). The impedance measurements were carried out in a frequency range of 100 KHz to 0.01 Hz with an AC amplitude of 10 mV at the open circuit potential ( $E_{corr}$ ) for different immersion times up to 60 days. ZSIme 3.22d software was used to interpret the data.

## RESULTS AND DISCUSSION

### WAXD Analysis

The WAXD patterns of cloisite 30B<sup>®</sup>, PCNA, and the EPCNA coating are shown in Figure 1. The patterns show a characteristic diffraction peak at  $18.2\text{ \AA}$  for pure cloisite 30B (Figure 1-a) and a peak with a  $d$ -spacing of  $26.7\text{ \AA}$  for PCNA (Figure 1-b). For the PCNA sample, due to the high surface energy of clay platelets and high polarity, butyl glycol and PANi nanoparticles are

adsorbed on clay platelets and consequently diffuse into the clay galleries; thus an increase in the basal spacing of clay platelets happens. In hardener-PCNA mixture, the hardener diffusion into the clay gallery is facilitated due to the presence of alkyl ammonium cations, the OH groups on clay plates, and the primary and secondary amine groups of the hardener chain. Therefore, when the hardener was mixed with PCNA, the peak shifted to lower angles [13-15, 23]. In the XRD analyzing of the EPCNA coating (Figure 1-C), the peak attributed to the basal spacing of the clay platelets increased further and showed that the clay was exfoliated.

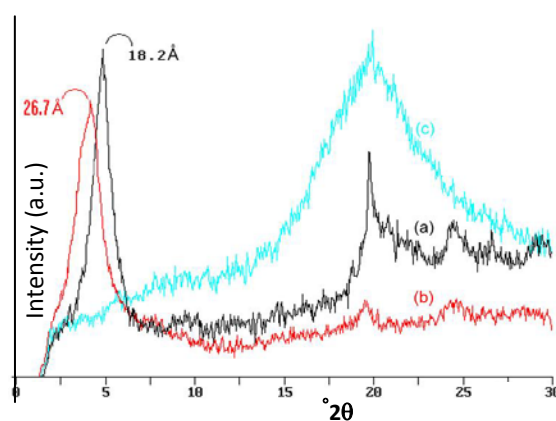


Figure 1: The XRD patterns (a) Cloisite 30B, (b) PCNA, and (c) EPCNA coating

### Particle Size Investigation

#### Dynamic Light Scattering

The particle size was determined by dynamic light scattering for the hardener containing nanopolyaniline. To reduce the particle size and make particles less agglomerated, the received polyaniline was first dispersed in ethanol using an ultrasound homogenizer. The prepared mixture was added to the hardener and the particle size was confirmed by DLS. As it is shown in Figure 2, a sample with a particle size of 50.7 nm with the maximum intensity was prepared.

#### TEM Analysis

The TEM images obtained from the organo-

modified clay exhibited a good dispersion of clay platelets in the EPCNA coating. As shown in Figure 3(a), EPCNA showed that the lamellar nanocomposite material had a mixed nanomorphology. The individual silicate layers, along with multiple layer stacks, were found to be exfoliating in the polymeric matrix.

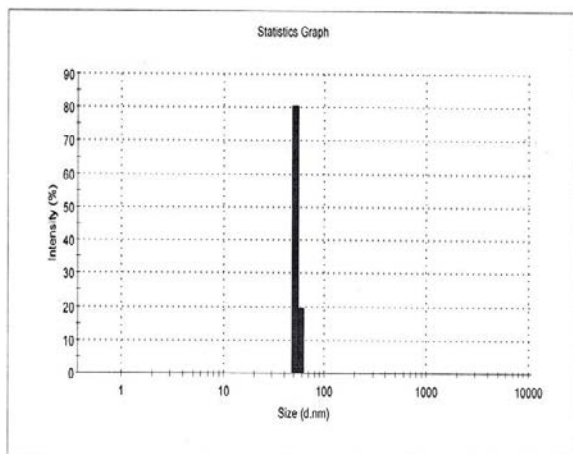


**Figure 2: Particle size statistics by intensity in the hardener**

In addition, some larger intercalated tactoids (multiple layer particles) can be identified. The TEM images also showed that PANi nanoparticles (30-50 nm) had been penetrated between clay platelets with a good dispersion in EPCNA dry film (Figure 3-a). Moreover, NanoPANi was finely distributed in the ENPN coating sample with a particle size of 30-50 nm (Figure 3-b). It is apparent that the prepared nanoadditives have proper compatibility with the coating with no phase separation.

### SEM Analysis

Scanning electron microscopy technique was used for studying metal coating interface. The formation of a stable iron oxide layer at the interface of the coating containing polyaniline and iron metal has been reported by some authors [24-26]. The scanning electron micrographs of the samples ENPN and EPCNA shown in Figures 4a and 4b agree with the formation of stable iron oxide layer suggested by the abovementioned

authors. Furthermore, comparing the cross-sections micrographs of the coated samples shows that using PCNA nanoadditive in the coating film results in the formation of a uniform and dense oxide layer at the metal-coating interface.

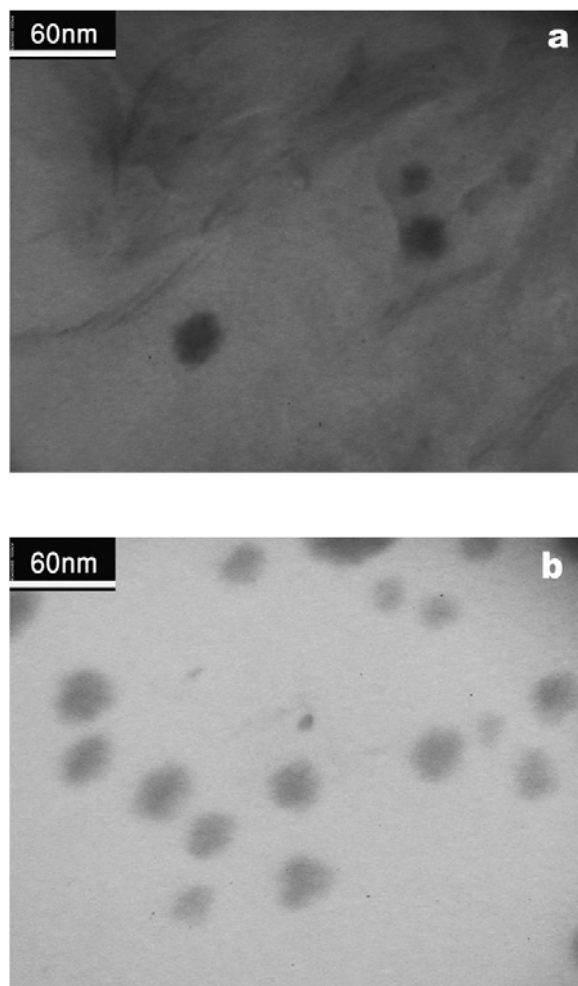


**Figure 3; TEM of the final dried film (a) EPCNA and (b) ENPN**

This formed oxide layer can be attributed to the presence of nanoclay particles and the reduction of the diffusion of water and other aggressive species to the coating film.

### Corrosion Resistance Tests

#### Salt Spray Test

Figure 5 shows the coated samples after 60 days exposure in a salt spray fog chamber. Size, distribution, and blister frequency on the coatings

surfaces were reported according to ASTM D714 (Table 3).

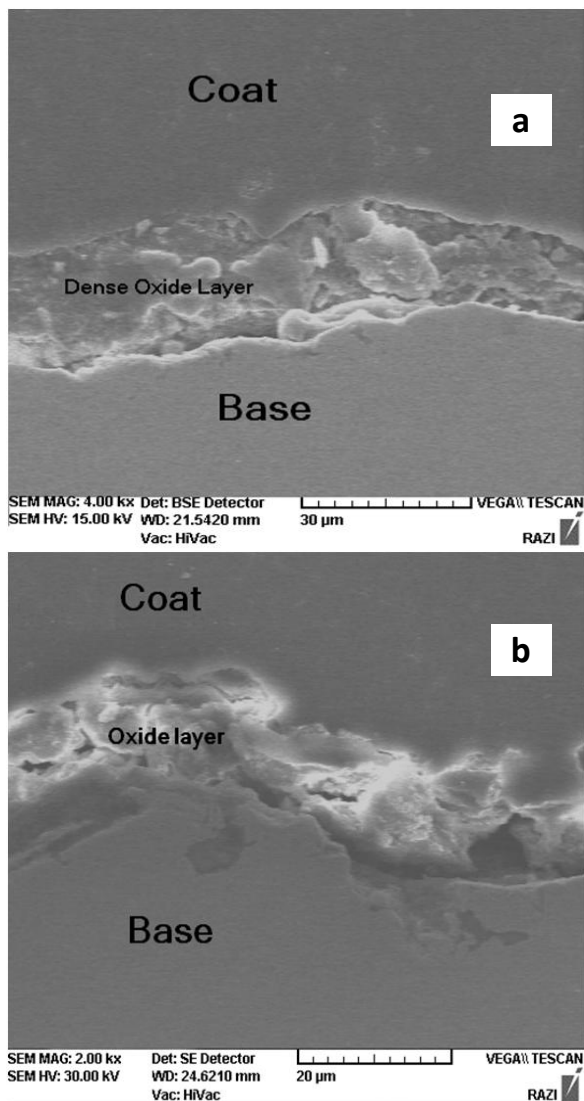


Figure 4: SEM of metal-coating interface (a) EPCNA and (b) ENPN

After 60 days exposure in an aggressive medium, blister size No. 2 with low blister frequency was observed in the ENPN sample around the scratched area and no rust was found under the blisters as a result of the formation of the stable oxide layer on the metal surface [5]. In case of EPCNA, no damage was observed on the surface of the coating film. This can be attributed to the use of PANi and clay nanoparticles in the coating film and the dense stable oxide layer formed on the metal surface, which results in an improvement to physicomechanical properties

of the coating [4,27].

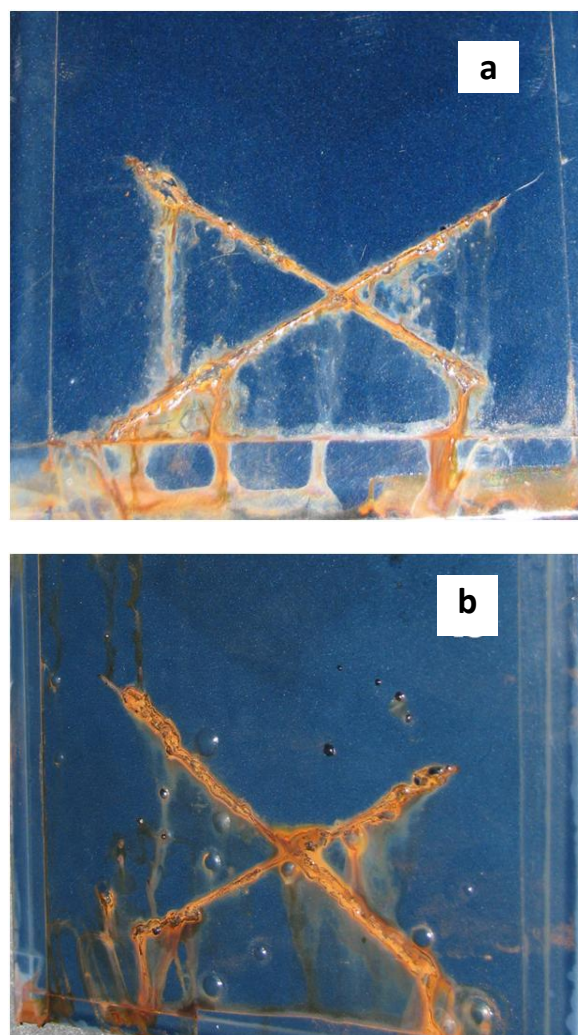


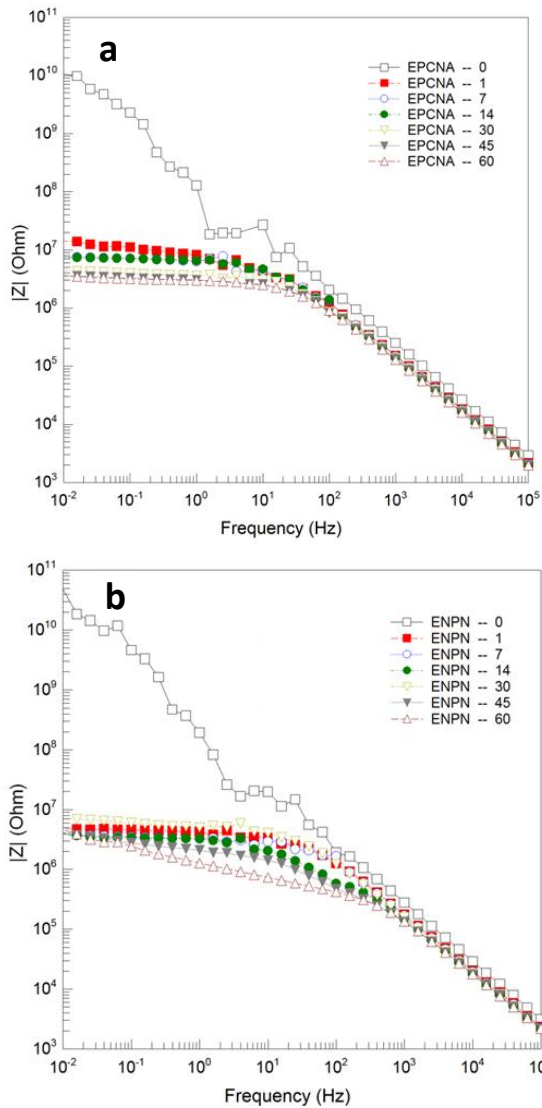
Figure 5: Surface appearance of the samples after exposing to salt spray for 60 days (a) EPCNA and (b) ENPN

Table 3: Results of salt spray according to ASTM D714

Coating	Blister frequency		Blister size No.	
	On the scratch	Around scratch	On the scratch	Around scratch
EPCNA	few	no blister	8	no blister
ENPN	medium	few	6	2-4

### Electrochemical Impedance Spectroscopy (EIS) Studies

The impedance behavior of the EPCNA and ENPN coating samples is shown in Figure 6.



**Figure 6: Bode plots at different times for (a) EPCNA and (b) ENPN**

The analysis of typical Bode diagrams suggests that two different equivalent circuit models are required to model the results. The Randles circuit was used at the initial time of immersion (Figure 7-a), but after 1 day of immersion, the EIS data were modeled with the porous film model (Figure 7-b).

The variations of coating resistance ( $R_c$ ), charge transfer resistance ( $R_{ct}$ ), water uptake, and corrosion potential ( $E_{corr}$ ) with time are presented in Table 4 for the EPCNA and ENPN coatings. The water uptake values of the samples shown in Table 4 obtained from Brasher–Kingsbury equation as given by:

$$Water\ uptake = \frac{\log(C_t/C_0)}{\log 80} \quad (1)$$

where,  $C_t$  is the electrical capacitance of the coating during  $t$  time of immersion and  $C_0$  stands for the electrical capacitance of the coating before immersion [32].

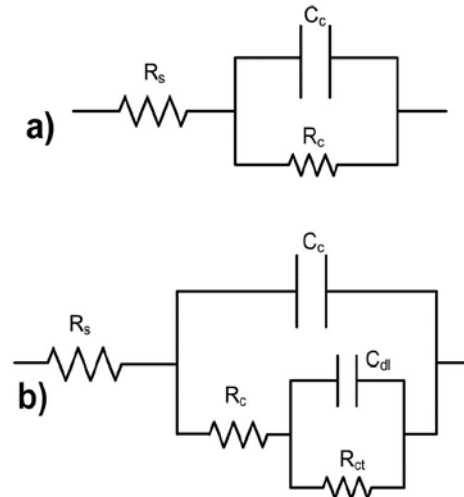


**Figure 7: Equivalent circuit for the impedance of coated steel**

The EIS data resulting from the specimens at initial immersion in a 3.5 wt.% NaCl solution (Figure 6) show an extremely high resistance ( $R_c$ ) for the coatings indicating that the coating acts almost as a perfect capacitor. It means that there is not enough water diffusion to the structure of films.

After one day of immersion, the coating resistance of EPCNA ( $R_c$ ) was  $3.053 \times 10^6 \Omega\text{cm}^2$  and continued to be  $3.01 \times 10^6 \Omega\text{cm}^2$  after 60 days of immersion. Therefore, there was no obvious change in  $R_c$  of EPCNA. However, in the ENPN sample with 60 days of immersion, the  $R_c$  value ( $4.13 \times 10^5 \Omega\text{cm}^2$ ) is much lower than its initial state (Table 4).

The  $R_c$  of the coatings at the initial step mainly depends on the nature and thickness of the coating, but during the immersion period, the EIS results showed that the sample coated by EPCNA provided a better barrier protection than the one coated by ENPN.

Table 4: Impedance parameters of coating samples

Time (day)	ENPN				EPCNA			
	$R_C$ ( $\Omega\cdot\text{cm}^2$ )	$R_{Ct}$ ( $\Omega\cdot\text{cm}^2$ )	Water Uptake (%)	$E_{corr}$ (mV vs. SCE)	$R_C$ ( $\Omega\cdot\text{cm}^2$ )	$R_{Ct}$ ( $\Omega\cdot\text{cm}^2$ )	Water Uptake (%)	$E_{corr}$ (mV vs. SCE)
initial	1.68E11	-	-	-55	1.855E10	-	-	-114
1	2.60E6	1.94E6	0.146	-401	3.053E6	8.11E6	0.092	-283
7	3.16E6	5.93E5	0.152	-346	2.91E6	4.22E6	0.097	-327
14	6.03E5	2.71E6	0.157	-548	2.33E6	4.50E6	0.100	-288
30	4.50E5	3.42E6	0.161	-315	2.51E6	3.69E6	0.101	-341
45	4.86E5	2.35E6	0.163	-599	2.63E6	3.08E6	0.103	-328
60	4.13E5	1.01E6	0.170	-378	3.01E6	3.00E6	0.104	-244

In the EPCNA coating film, due to using PCNA nanoadditive and the presence of the nanoclay particles (Figure 3-a), the length of the diffusion pathway increases and thus the permeability of the coating decreases and ultimately the barrier effect improves in EPCNA (Figure 4-a). The water uptake values of the coatings confirm the barrier effect of nanoclay in EPCNA, and therefore, the water uptake of the EPCNA sample is much less than that of ENPN (Figure 8).

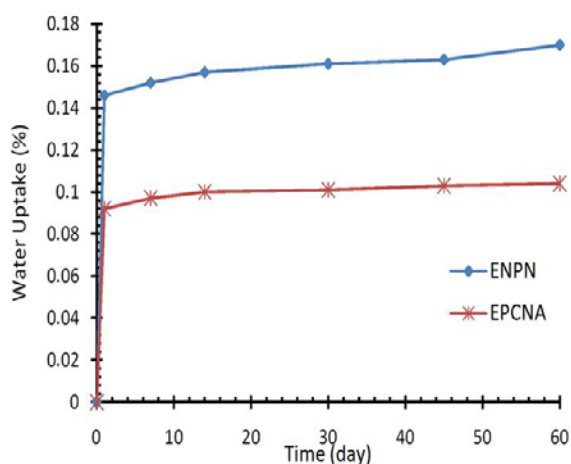


Figure 8: Water uptake curve for the coating samples after 60 days

The coating containing PCNA nanoadditive, due to having PANi, can cause continuous protection by exchanging electrons with the metallic substrate. The electrons produced by the oxidation of the metal at a corrosion site flow to the surrounding metal surface and are consumed by a redox reaction. Using PANi in the mentioned coating

causes the electro-chemical reaction to occur differently during the localized corrosion. This could be due to the use of PANi, which leads to the stabilization of the metal potential in the passive regime and results in the formation of a stable oxide layer on the metal surface (Figure 4). Additionally, PANi captures the chlorine ions that cause pitting corrosion by the destruction of the passivating layer [5, 6, 28-31].

The charge transfer resistances ( $R_{Ct}$ ) of EPCNA and ENPN (Figure 7 and Table 4) are  $5.44 \times 10^6 \Omega\text{cm}^2$  and  $1.30 \times 10^6 \Omega\text{cm}^2$  respectively at the beginning of immersion in the solution. The high  $R_{Ct}$  values of the coating samples indicate that the charge transfer reactions and corrosion process at the metal surface are improved. This is due to the presence of NanoPANi in the coating films.

After seven days of immersion, a significant reduction of  $R_{Ct}$  in EPCNA, as compared with ENPN (Figure 9), could be related to the presence of clay plates between PANi particles in the coating film. This phenomenon can reduce PANi particle conductivity in polymeric matrix and possibly affect the passive layer formation on the metal surface; however, for ENPN, the oxide layer formation will improve during the immersion time.

After 30 days of immersion,  $R_{Ct}$  of EPCNA and ENPN were  $2.92 \times 10^6 \Omega\text{cm}^2$  and  $3.53 \times 10^6 \Omega\text{cm}^2$  and after 60 days those were  $3.00 \times 10^6 \Omega\text{cm}^2$  and  $5.31 \times 10^5 \Omega\text{cm}^2$  respectively. As shown in

Figure 9, in the interval of 30 to 60 days, the  $R_{ct}$  attain to a steady state in EPCNA, while it falls in ENPN.

It seems that the presence of the NanoPANI particles between the clay platelets causes a reduction in permeability and possibly the formation of dense stable oxide layer on the metal surface simultaneously (Figure 4-a).

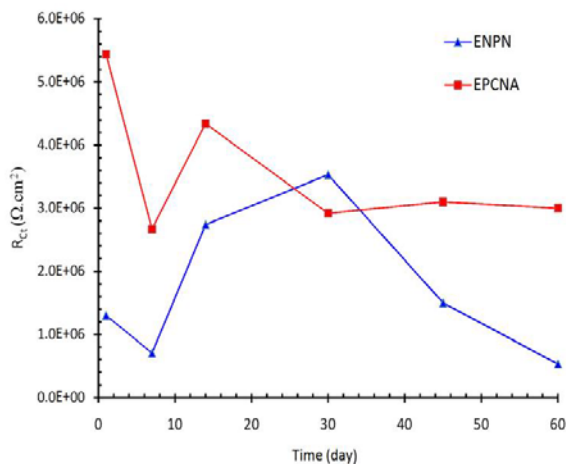


Figure 9:  $R_{ct}$  variation of the coating samples

The changes of the coating samples  $E_{corr}$  (Table 4 and Figure 10) indicate that a stable oxide layer is formed on the metal surface. The  $E_{corr}$  fluctuations of ENPN have been attributed to the formation, failure, and repairing of the formed oxide layer on the metal surface due to using dispersed PANi nanoparticles in the coating film. In fact, the cyclic catalytic redox property of PANi leads to the formation and repair of the oxide layer on the metal surface, but its failure is due to the penetration of corrosive ions [5, 6, 27-31]. After 60 days of immersing the EPCNA sample,  $E_{corr}$  was -244 mV (vs. SCE), which mentioned the steady state earlier.

The presence of PANi and clay nanoparticles together in the coating results in the formation of a dense stable oxide layer with less permeability and more corrosion protection (Figure 4-a and Figure 6).

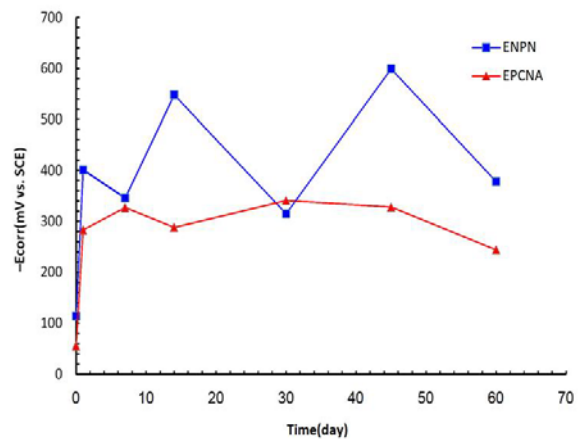


Figure 10: Corrosion potential ( $E_{corr}$ ) of the coatings as a function of immersion time

## CONCLUSIONS

Nanoadditives can be used to improve the anticorrosion properties of epoxy coatings. PCNA nanoadditive was prepared by a direct mixing method using 3 wt.% Cloisite 30B and 0.03 wt.% NanoPANI. The characterization results showed that the clay was exfoliated and its use caused improved barrier properties. Also, the particle size range of polyaniline was between 30 and 60 nm with a good distribution in hardener and final dry film, which causes a better anticorrosion effect. The use of PCNA in the epoxy coating lead to an increase in the corrosion resistance, which could be due to the formation of a dense stable oxide layer in the metal coating interface. Finally, more positive  $E_{corr}$ , higher  $R_C$  and  $R_{ct}$ , and less water uptake revealed better protective performance for the EPCNA coating compared to the ENPN coating.

## REFERENCES

- [1] Bhupesh M. and Abhishek K., "Nano additives: A Review," *Paintindia*, **2008**, *58*, 113-132.
- [2] Sawitowski T., "Nano and Hybrid Coatings Conference," Manchester, UK, **2005**.
- [3] Yeh J. M. and Chang K. C., "Polymer/layered Silicate Nanocomposite Anticorrosive Coatings," *J. Ind. Eng. Chem.*, **2008**, *14*, 275-291.

- [4] Bagherzadeh M. R. and Mahdavi F., "Preparation of Epoxy-clay Nanocomposite and Investigation on its Anti-corrosive Behavior in Epoxy Coating," *Prog. Org. Coat.*, **2007**, *60*, 117-120.
- [5] Bagherzadeh M. R., Ghasemi M., Mahdavi F., and Shariatpanahi H., "Investigation on Anticorrosion Performance of Nano and Micro Polyaniline in New Water-based Epoxy Coating," *Prog. Org. Coat.*, **2011**, *72*, 348-352.
- [6] Bagherzadeha M. R., Mahdavi F., Ghasemi M., Shariatpanahi H., et al., "Using Nano-emeraldine Salt-polyaniline for Preparation of a New Anticorrosive Water-based Epoxy Coating," *Prog. Org. Coat.*, **2010**, *68*, 319-322.
- [7] Chen F. and Liu P., "Conducting Polyaniline Nanoparticles and their Dispersion for Waterborne Corrosion Protection Coatings," *Appl. Mater. Interfaces*, **2011**, *3*, 2694-2702.
- [8] Khan M. I., Chaudhry A. U., Hashim S., Zahoor M. K., et al., "Recent Developments in Conductive Polymer Coatings for Corrosion Protection," *Chem. Eng. Res. Bull.*, **2010**, *14*, 73-86.
- [9] Pavlidou S. and Papaspyrides C. D., "A Review on Polymer-layered Silicate Nanocomposites," *Prog. Polym. Sci.*, **2008**, *33*, 1119-1198.
- [10] Akbarinezhad E., Ebrahimi M., and Sharif F., "Synthesis of Exfoliated Polyaniline-clay Nanocomposite in Supercritical CO<sub>2</sub>," *J. Supercrit. Fluid*, **2011**, *59*, 124-130.
- [11] Olad A. and Rashidzadeh A., "Reparation and Anticorrosive Properties of PANI/Na-MMT and PANI/O-MMT Nanocomposites," *Prog. Org. Coat.*, **2008**, *62*, 293-298.
- [12] Kataria D., "Polyaniline Clay-polyimide Hybrid Nanocomposite Coatings for Corrosion Protection of AA 2024," M.S. Thesis, University of Cincinnati, USA, **2005**.
- [13] Chen Y., Wang X. H., Li J., Lu J. L., et al., "Polyaniline for Corrosion Prevention of Mild Steel Coupled with Copper," *Electrochim. Acta.*, **2007**, *52*, 5392-5399.
- [14] Yeh J. M., Liou S. J., Lai C. Y., Wu P. C., et al., "Enhancement of Corrosion Protection Effect in Polyaniline via the Formation of Polyaniline-clay Nanocomposite Materials," *Chem. Mater.*, **2001**, *13*, 1131-1136.
- [15] Song D. H., Lee H. M., Lee K. H., and Choi H. J., "Intercalated Conducting Polyaniline-clay Nanocomposites and their Electrical Characteristics," *J. Phys. Chem. Solids*, **2008**, *69*, 1383-1385.
- [16] Sudha J. D. and Sasikala T. S., "Studies on the Formation of Self-assembled Nano/microstructured Polyaniline-clay Nanocomposite (PANICN) using 3-Pentadecyl Phenyl Phosphoric Acid (PDPPA) as a Novel Intercalating Agent Cum Dopant," *Polymer*, **2007**, *48*, 338-347.
- [17] Yoshimoto S., Ohashi F., Ohnishi Y., and Nonami T., "Synthesis of Polyaniline-montmorillonite Nanocomposites by the Mechanochemical Intercalation Method," *Synthetic Met.*, **2004**, *145*, 265-270.
- [18] Soto-Oviedo M. A., Araújo O. A., Faez R., Mirabel C., et al., "Antistatic Coating and Electromagnetic Shielding Properties of a Hybrid Material Based on Polyaniline/organoclay Nanocomposite and EPDM Rubber," *Synthetic Met.*, **2006**, *156*, 1249-1255.
- [19] Jang J., Bae J., and Lee K., "Synthesis and Characterization of Polyaniline Nanorods as Curing agent and Nanofiller for Epoxy Matrix Composite," *Polymer*, **2005**, *46*, 3677-3684.
- [20] Bhadra S., Khastgir D., Singha N. K., and Lee J. H., "Progress in Preparation, Processing and Application of Polyaniline," *Prog. Polym. Sci.*, **2009**, *34*, 783-810.
- [21] Hoang H. V. and Holze R., "Electrochemical Synthesis of Polyaniline/Montmorillonite Nanocomposites and their Characterization," *Chem. Mater.*, **2006**, *18*, 1976-1980.
- [22] Hosseini M. G., Raghbi-Boroujeni M., Ahadzadeh I., Najjar R., et al., "Effect of Polypyrrole-montmorillonite Nanocomposites Powder Addition on Corrosion Performance of Epoxy Coatings on Al 5000," *Prog. Org. Coat.*, **2009**, *66*, 321-327.

- [23] Kiliaris P. and Papaspyrides C. D., "Polymer/layered Silicate (Clay) Nanocomposites: An Overview of Flame Retardancy," *Prog. Polym. Sci.*, **2010**, *35*, 902-958.
- [24] Twite R. L. and Bierwagen G. P., "Review of Alternatives to Chromate for Corrosion Protection of Aluminum Aerospace Alloys," *Prog. Org. Coat.*, **1998**, *33*, 91-100.
- [25] Kinlen P. J., Silverman D. C., and Jeffreys C. R., "Corrosion Protection using Polyaniline Coating Formulations," *Synth. Met.*, **1997**, *85*, 1327-1332.
- [26] Saravanan K., Sathiyarayanan S., Muralidharan S., Syed Azim S., et al., "Performance Evaluation of Polyaniline Pigmented Epoxy Coating for Corrosion Protection of Steel in Concrete Environment," *Prog. Org. Coat.*, **2007**, *59*, 160-167.
- [27] Podsiadlo P., Shim B. S., and Kotov N. A., "Polymer/clay and Polymer/carbon Nanotube Hybrid Organic-inorganic Multilayered Composites made by Sequential Layering of Nanometer Scale Films," *Coordin. Chem. Rev.*, **2009**, *253*, 2835-2851.
- [28] Armelin E., Pla R., Liesa F., Ramis X., et al., "Corrosion Protection with Polyaniline and Polypyrrole as Anticorrosive additives for Epoxy Paint," *Corros. Sci.*, **2008**, *50*, 721-728.
- [29] Akbarinezhada E., Ebrahimi M., Sharif F., Attar M. M., et al., "Synthesis and Evaluating Corrosion Protection Effects of Emeraldine Base PAni/clay Nanocomposite as a Barrier Pigment in Zinc-rich Ethyl Silicate Primer," *Prog. Org. Coat.*, **2011**, *70*, 39-44.
- [30] Saravanan K., Sathiyarayanan S., Muralidharan S., Syed Azim S., et al., "Performance Evaluation of Polyaniline Pigmented Epoxy Coating for Corrosion Protection of Steel in Concrete Environment," *Prog. Org. Coat.*, **2007**, *59*, 160-167.
- [31] Sathiyarayanan S., Muthukrishnan S., and Venkatachari G., "Performance of Polyaniline Pigmented Vinyl Acrylic Coating on Steel in Aqueous Solutions," *Prog. Org. Coat.*, **2006**, *55*, 5-10.
- [32] Castela A. S. L., Simoes A. M., and Ferreira M. G. S., "E. I. S. Evaluation of Attached and Free Polymer Films," *Prog. Organ. Coat.*, **2000**, *38*, 1-7.